

PAPER • OPEN ACCESS

## Influence of the axial compressor blade row defects on the industrial gas turbine performance

To cite this article: V L Blinov and I S Zubkov 2020 *J. Phys.: Conf. Ser.* **1683** 042049

View the [article online](#) for updates and enhancements.



The Electrochemical Society  
Advancing solid state & electrochemical science & technology  
2021 Virtual Education

**Fundamentals of Electrochemistry:**  
Basic Theory and Kinetic Methods  
Instructed by: **Dr. James Noël**  
Sun, Sept 19 & Mon, Sept 20 at 12h–15h ET

Register early and save!



# Influence of the axial compressor blade row defects on the industrial gas turbine performance

V L Blinov and I S Zubkov

Yeltsin UrFU,

Russia, 620002 Ekaterinburg, Mira, 19

v.l.blinov@urfu.ru

**Abstract.** This paper presents the compressor blade algorithm for predicting the defect influence on the characteristics of the stage, axial compressor or GTU as a whole. The developed model is based on the use of Bezier curves, with the control point coordinates calculated using the main geometric parameters of the airfoil, which provides highly precise geometry of both the airfoil and the blade as a whole. The paper shows some results of verification of the developed method and the selected numerical model parameters, as well as the analysis of the defect influence on the airfoil flow conditions in order to demonstrate the capabilities of the algorithm. The main results of the study were summarized and recommendations for further research were developed.

## 1. Introduction

Currently, the application range of gas turbine technologies tends to widen including transport (air and maritime) and various industries (chemical, oil and gas) [1]. In addition, gas turbines are increasingly being used in power industry, e.g. in the combined steam and gas cycle at thermal power plants. In modern combined-cycle plants, a gas turbine unit (GTU) generates more than half of the output power. At the same time, gas turbine operating parameters substantially contribute to the overall reliability and efficiency.

The GTU efficiency largely depends on the technical condition of its components, which can be changed significantly while in operation [2]. GTU technical condition determines its service limit [3]. One of the most complex and important GTU components is an axial compressor. The axial compressor consumes more than half of the power generated by the turbine, which depends on the pressure ratio in the cycle, turbo-machine efficiency, incoming gas temperature (before it goes to the turbine), and incoming air temperature (before it goes to the compressor). Since the axial compressor consumes a large amount of power, it is important to achieve and maintain its high efficiency and sufficient gas-dynamic stability margin, which primarily depend on the quality of the blade row [4]. In this regard, allowable size and shape deviations are specifically regulated during manufacturing and repair of axial compressor blades, as well as other turbines [5, 6]. Significant geometric deviations from the reference or allowable values may lead to various turbine breakdowns. Thus, making a blade leading edge thinner (in other words, reducing its radius) will result in a significant margin reduction of the axial compressor stable operation in variable operating modes, as well as in the loss of the blade strength characteristics [7]. However, at the same time, this defect is relatively beneficial – with a thinner leading edge, the edge losses will be lower, which will improve the stage efficiency when operating at rated mode [2, 4]. Reducing the maximum airfoil thickness may serve as another example



Content from this work may be used under the terms of the [Creative Commons Attribution 3.0 licence](https://creativecommons.org/licenses/by/3.0/). Any further distribution of this work must maintain attribution to the author(s) and the title of the work, journal citation and DOI.

[8]. The negative impact of this factor is related to the blade channel deformation, which leads to changes in the flow parameters near the airfoil and can result in local failures and, in some cases, in the blade strength and dynamic characteristic degradation. On the other hand, the level of friction loss may decrease due to the reduced friction area. Such deviations that are contradictory in their impact on the axial compressor efficiency may concern almost all airfoil geometric parameters, so the assessment and analysis of such an impact is an important and long-term task. The operating mode of the stage should be seriously considered, since it will be the factor determining the nature of the defect influence on the main parameters of the axial compressor operation [4, 9].

There are three types of blade defects according to their causes: structural (for example, the presence of stress concentrators), technological (usually caused by a deviation from the optimal blade production process), and operational (corrosion and erosion processes, deviations from the rated duty, etc.). According to the statistics in [10], 29% of defects are structural, 17% and 11% – technological and operational, respectively, while the remaining 43% of defects are caused by a combination of those factors. However, a number of researchers (e.g. [11]), still consider operational defects (often blade erosion) the primary reason of rated mode deviations and GTU breakdowns. The development of certain defects will greatly depend on the scheme of the gas turbine, the degree of design solution testing and operating conditions.

Today, 3D scanning is the main tool used to create models of defective blades (as an element of reverse engineering). In fact, the quality of a manually created or virtual three-dimensional model of an object may not always meet the problem setting, while 3D scanning allows achieving higher precision by using the real object, which is emphasized in [8]. However, the use of this method is limited due to related expenses (an expensive 3D scanner, a set of positioning targets, and other additional equipment) and the possible lack of access to the object under study. The development of completely digital models that would allow to predict accurately the performance of a gas turbine with defective components of geometric deviations in its design is a quite promising task. That is why many machine-building enterprises are actively engaged in researches in this field.

## 2. Developed Method

This research is aimed at developing a mathematical model that allows to predict the influence of a particular geometric deviation of the blade on the characteristics of the axial compressor and GTU as a whole with a reasonable degree of accuracy (figure 1). At the initial stage of creating this model, the main task is to develop a mathematical description of the blade, which would not only ensure the accuracy of its design, but also allow to make significant changes to the shape of the blade in all its regions and sections. In the future, the developed geometric topology will be applied to create a computational model used for numerical simulation of the working fluid flow in the air-gas channel containing defective blades. A database will be formed from the results obtained. If there were any defects in certain components of the air-gas channel, the user would get accurate information on the GTU compressor performance by setting specific parameters of the defect (for example, the value of the airfoil chord in the periphery). Similarly, a mathematical model determining the influence of defects on the blade strength characteristics can be developed. The tasks of the enterprises manufacturing, repairing and operating GTUs include the creation of a primary mathematical model, its implementation, and gradual refinement (based on up-to-date information).

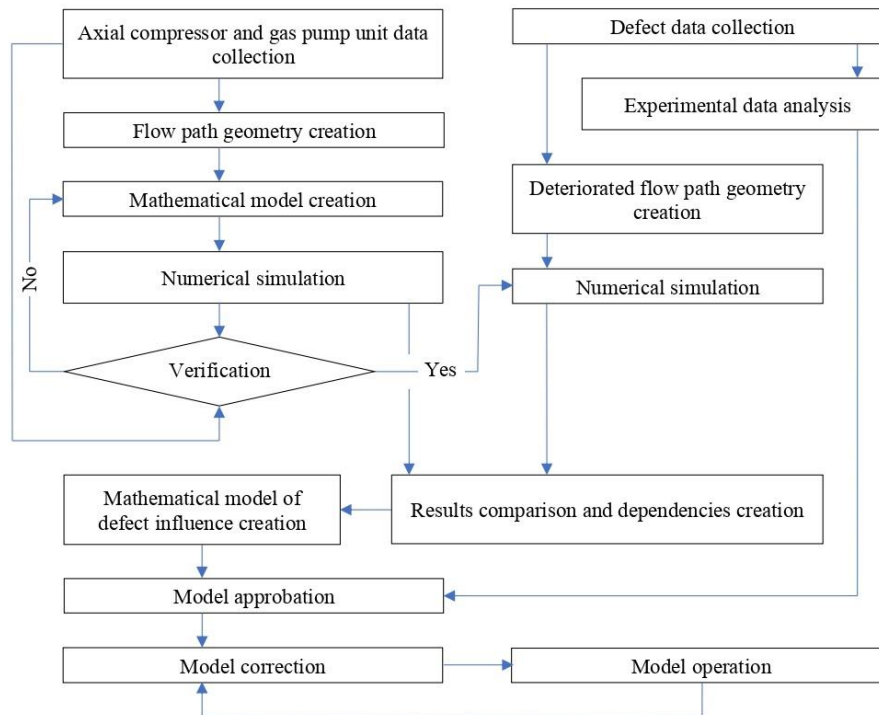


**Figure 1.** Defect influence model algorithm

The developed mathematical description of the blade geometry uses various Bezier curves (figure 2, a): second-order Bezier curves for edge modelling (1), and third-order Bezier curves for the suction and pressure sides of the blade (2). In this case, the airfoil coordinates are determined using the following equations:

$$\begin{aligned}
 X_{lead} &= (1-t)^2 X_{B_3}^{ss} + 2t(1-t)X_{A_1} + t^2 X_{B_0}^{ps} \\
 Y_{lead} &= (1-t)^2 Y_{B_3}^{ss} + 2t(1-t)Y_{A_1} + t^2 Y_{B_0}^{ps} \\
 X_{trail} &= (1-t)^2 X_{B_0}^{ss} + 2t(1-t)X_{A_2} + t^2 X_{B_3}^{ps} \\
 Y_{trail} &= (1-t)^2 Y_{B_0}^{ss} + 2t(1-t)Y_{A_2} + t^2 Y_{B_3}^{ps}
 \end{aligned} \tag{1}$$

$$\begin{aligned}
 X_{ss} &= (1-t)^3 X_{B_0}^{ss} + 3t(1-t)^2 X_{B_1}^{ss} + 3t^2(1-t)X_{B_2}^{ss} + t^3 X_{B_3}^{ss} \\
 Y_{ss} &= (1-t)^3 Y_{B_0}^{ss} + 3t(1-t)^2 Y_{B_1}^{ss} + 3t^2(1-t)Y_{B_2}^{ss} + t^3 Y_{B_3}^{ss} \\
 X_{ps} &= (1-t)^3 X_{B_0}^{ps} + 3t(1-t)^2 X_{B_1}^{ps} + 3t^2(1-t)X_{B_2}^{ps} + t^3 X_{B_3}^{ps} \\
 Y_{ps} &= (1-t)^3 Y_{B_0}^{ps} + 3t(1-t)^2 Y_{B_1}^{ps} + 3t^2(1-t)Y_{B_2}^{ps} + t^3 Y_{B_3}^{ps}
 \end{aligned} \tag{2}$$

In equations (1) and (2)  $t \in [0, 1]$  – the parameter that determines the position of a point on the Bezier curve. In this work, the setting unit for the suction and pressure sides of the blade is 0.01 and 0.04 for the edges, which allows calculating the coordinates of 100 and 25 points, respectively.

The coordinates of the control points ( $B_0, B_1, B_2, B_3$ ) of the curves describing the leading and trailing edge as well as the suction and pressure sides of the blade are calculated using the main geometric parameters of the airfoil – pitch angle ( $\beta_y$ ), chord ( $b$ ), radii of the leading and trailing edge ( $R_{in}$ ;  $R_{out}$ ) and edge angles ( $\varphi_1$ ;  $\varphi_2$ ), inlet and outlet blade angles ( $\beta_{1b}$ ;  $\beta_{2b}$ ). This approach ensures highly precise design of the initial airfoil and provides the possibility to flexibly change its geometry [12]. Other geometric parameters of the airfoil (e.g. the maximum thickness) are calculated so that they could be controlled. The similar approach has proven itself in solving airfoil optimization problems [15, 16].

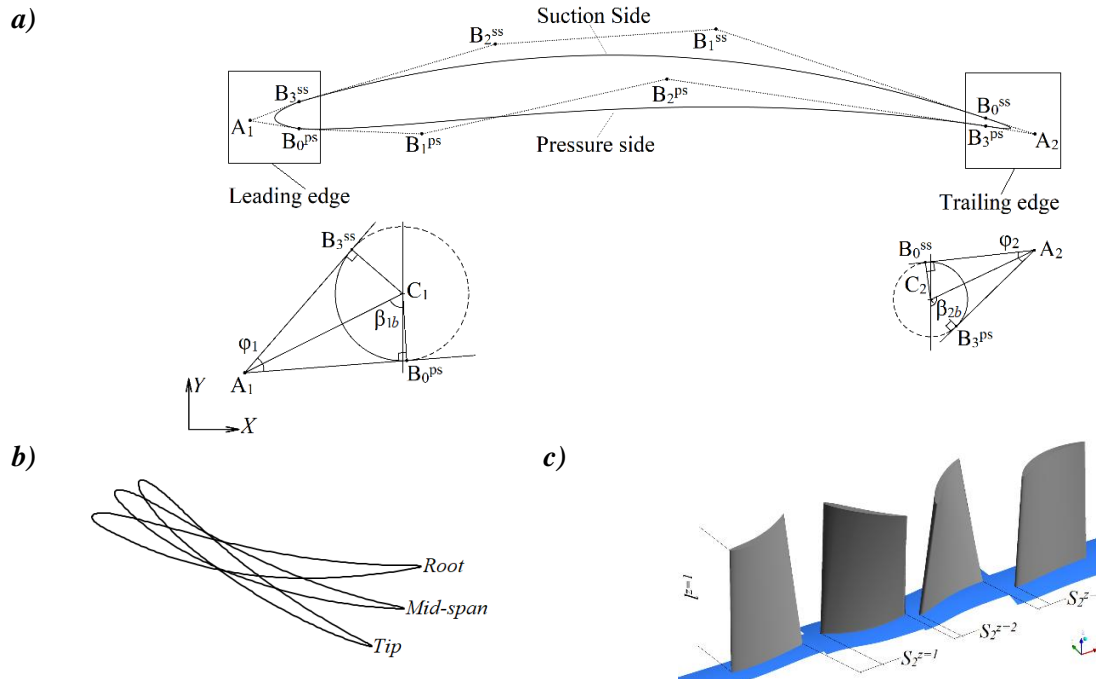


**Figure 2.** Design of the airfoil (a), blade (b) and air-gas channel (c) of an axial compressor

Using the required number of airfoils, set to a certain radius, allows to design a blade of any geometric shape (figure 2, b). The algorithm provides for setting the airfoil offset along the  $x$  and  $y$  axes. The axial compressor air-gas channel is formed by placing the blade along the root line of the channel at a certain axial distance (figure 2, c). Thus, a set of defects and deviations of the axial compressor blade row is reconstructed using local changes in the airfoil geometry.

This study analyses the proposed approach. As an example, the geometry of the NACA 65 airfoils with known characteristics [13] was reproduced using the described topology. Numerical simulations were performed in an axisymmetric setting, so the blade was set at the maximum distance from the axis of calculated domain (1400 mm) in order to approximate the experimental conditions. The boundary conditions were set based on the principle of total pressure and temperature, flow direction at the inlet ( $P_1^* = 1300 \text{ Pa}$ ;  $T_1^* = 288 \text{ K}$ ;  $45^\circ$ ), and static pressure at the outlet  $P_2 = 786 \text{ Pa}$ , taking into account *Reference Pressure* = 100000 Pa. The static pressure value was assumed based on the conditions specified in the report [13]: flow velocity  $w = 95 \text{ ft/s} = 28,96 \text{ m/s}$  and Reynolds number  $Re = 245000$ . The inlet was located at a distance of one chord from the leading edge of the blade, and the outlet at a distance of three chords from the trailing edge. The blade height and pitch were assumed based on the solidity  $b/t = 1.0$ , their value was 127 mm, and the number of blades in the hub was equal to 72. The  $k$ -Epsilon turbulence model was chosen due to lower requirements for computing resources and better convergence while maintaining reasonable accuracy of the results [9]. The *Air Ideal Gas* model was used as the working fluid. The calculation results were compared with experimental data [13] on the distribution of the pressure coefficient along the airfoil at different angles of attack, as well as with the airfoil characteristics, including the angle of attack – flow turning angle relationship (figure 3). The pressure coefficient is defined as follows:

$$S = \frac{P^* - P}{P_1^{dyn}}, \quad (3)$$

where  $P^*$ —total pressure in the hub;  $P$ — static pressure at a point on the airfoil surface;  $P_1^{dyn}$ — dynamic pressure in the hub.

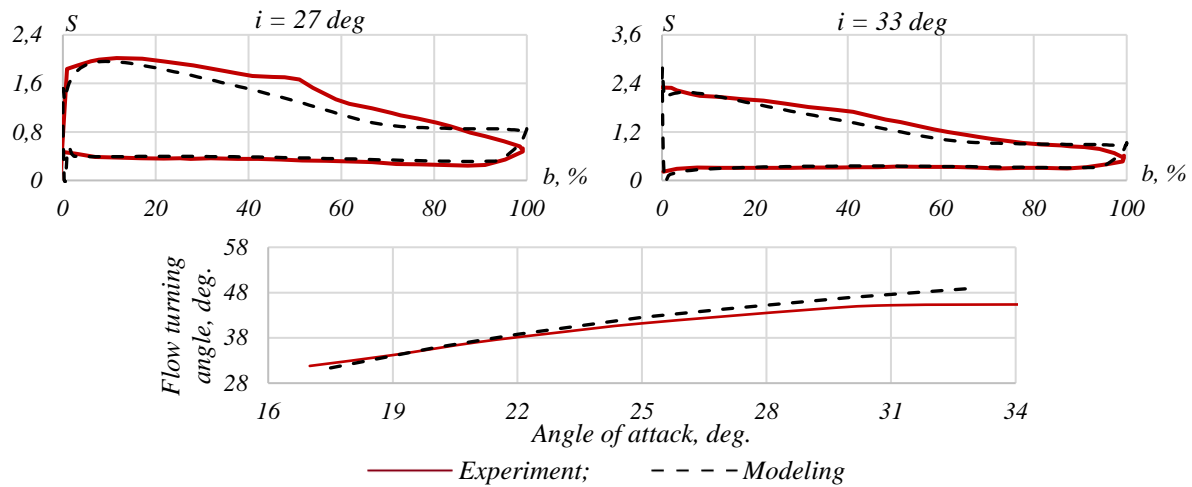


**Figure 3.** Comparison of experimental and calculated characteristics of the NACA 65-(27)10 airfoil

The calculated pressure distribution and characteristics of the NACA 65-(27)10 airfoil coincide with the experimental data with reasonable accuracy for this study. In this case, the observed deviations are due to the complexity of taking into account all the features of the experiment and the assumptions that idealize the numerical model (for example, the working fluid properties and the absence of surface roughness).

Figure 3 shows that the calculated values of the turning angle coincide with the experimental ones to the accuracy of up to 1% within the range of angles of attack  $i = 17 \dots 22^\circ$ . Greater deviation of the calculated data from the experiment at the angles of attack  $i > 22^\circ$  can be explained by a faster increase in the calculated value of the suction side flow separation compared to the experimental one, which led to a change in the value of the flow turning angle in the blade channel. The maximum deviation in the specified range was 7.1% (absolute) at the angle of attack  $i = 33^\circ$ . Similar results were obtained in [16].

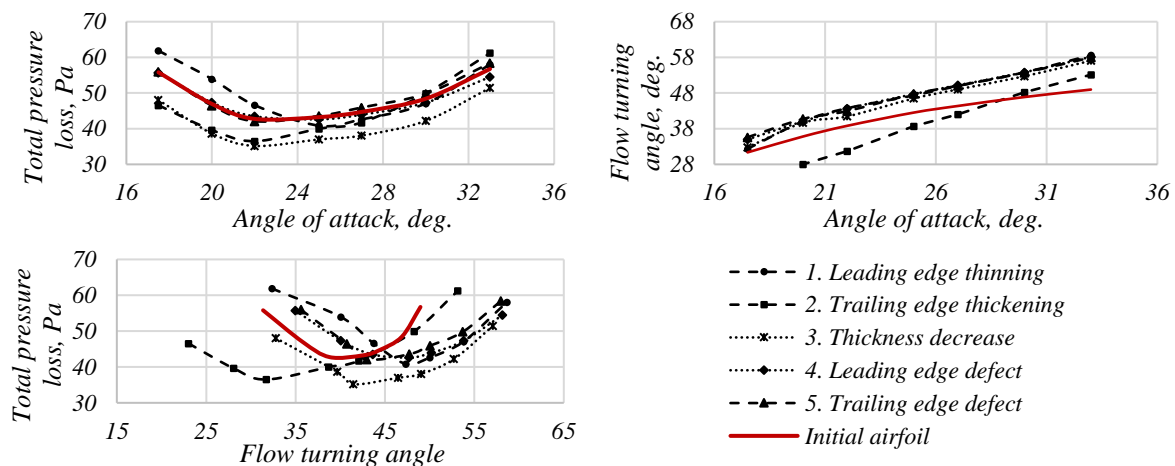
It should be emphasized that the task of computational model verification is an important stage of numerical simulation, but it is not the priority in this work. The main purpose of this study is to demonstrate the developed approach. The selected parameters of the computational model allow to conduct the research with relatively low requirements for computing resources and ensure reasonable accuracy of the results. For more detailed results of calculations on other types of airfoils, as well as recommendations on the parameters to choose for calculation models, see [12, 14, 16].

### 3. Results presentation

This paper studies five artificially created defects of the NACA 65-(27)10 airfoil, conventionally designated as the leading edge thinning, trailing edge thickening, thickness decrease, leading edge defect, and trailing edge defect. In fact, the changes made had an impact on several geometric parameters of the airfoil. The airfoil geometry was modified by changing the position of the control points of the Bezier curves (figure 2, a). All geometric parameters in accordance with the developed topology for the initial and defected airfoils are shown in table 1. The table also shows defected airfoil regions. “The angle of attack – total pressure loss – flow turning angle” characteristics were made based on the results of the calculations. They are shown in figure 4 together with the data for the initial airfoil.

**Table 1.** Created blade defects

№	Parameter (figure 2), units	Initial airfoil	Defected airfoil				
			— Initial airfoil region; - - - Defected airfoil region				
			1. Lead. edge thinning	2. Trail. edge thickening	3. Thickness decrease	4. Leading edge defect	5. Trailing edge defect
1	$B_0^{ss}(x; y)$ , mm	121.07; 5.64	121.07; 5.64	110.55; 12.10	121.07; 5.64	121.07; 5.64	121.07; 5.64
2	$B_1^{ss}(x; y)$ , mm	71.50; 40.00	71.50; 40.00	65.00; 37.00	71.50; 37.00	71.50; 40.60	71.50; 40.00
3	$B_2^{ss}(x; y)$ , mm	12.70; 22.06	12.70; 22.06	12.70; 22.06	12.70; 21.00	10.00; 21.00	12.70; 22.06
4	$B_3^{ss}(x; y)$ , mm	-0.074; 1.79	-0.074; 1.79	-0.074; 1.79	-0.074; 1.79	0.930; 1.79	-0.074; 1.79
5	$B_0^{ps}(x; y)$ , mm	1.98; 0.611	1.98; 0.611	1.98; 0.611	1.98; 0.611	2.98; 0.611	1.98; 0.611
6	$B_1^{ps}(x; y)$ , mm	30.00; 14.50	30.00; 14.50	30.00; 14.50	30.00; 17.00	30.00; 14.50	30.00; 14.50
7	$B_2^{ps}(x; y)$ , mm	97.50; 18.00	97.50; 18.00	90.00; 16.50	97.50; 19.00	97.50; 18.00	97.50; 18.00
8	$B_3^{ps}(x; y)$ , mm	120.42; 5.10	120.42; 5.10	112.29; 8.49	120.42; 5.10	120.42; 5.10	120.42; 5.10
9	$A_1(x; y)$ , mm	-0.953; -1.20	-3.00; -3.00	-0.953; -1.20	-0.953; -1.20	0.050; -1.20	-0.953; -1.20
10	$A_2(x; y)$ , mm	133.25; -5.37	133.25; -5.37	120.00; 6.50	133.25; -5.37	133.25; -5.37	136.00; -5.37
11	$R_{in}$ , mm	1.0	0.5	1.0	1.0	1.0	1.0
12	$R_{out}$ , mm	0.1	0.1	0.4	0.1	0.1	0.1
13	$\beta_{1b}$ , deg.	60	60	60	60	54	60
14	$\beta_{2b}$ , deg.	45	45	48	45	45	50
15	$b$ , mm	127	130	115	127	125	129
16	$C_{max}$ , mm	12.64	12.64	12.64	9.55	12.64	12.64

**Figure 4.** The airfoil characteristics based on defects

#### 4. Results analysis

The calculations performed prove that the proposed approach to the construction of the axial compressor blade row allows to describe various defects with sufficient flexibility by changing the position of the control points. Since the results of the airfoil description in the proposed method are the coordinates of the blade, it is possible, if necessary, to create complex local defects (e.g. nicks) by manually changing the coordinates. The defects discussed above lead to a change in the characteristics of the axial compressor airfoils. The geometric changes may turn positive or negative depending on the airfoil operating mode. The results obtained are in qualitative agreement with the theory [4].



When changing the shape of the leading edge (option 1, table 1), there is the decrease of total pressure losses by 1.0...5.5% in a certain optimal range of angles of attack  $i = 24 \dots 30^\circ$ . Beyond this range, losses increase, exceeding the initial airfoil losses by 9.8% and 4.1% at angle of attack values  $i = 17.5^\circ$  и  $33^\circ$ , respectively. The airfoil characteristics become steeper, and the range of stable operation is reduced due to the leading edge sharpening.

From the theoretical perspective, increasing the radius of the trailing edge should result in more losses due to worse blurring of the vortices behind the blade. Creating a similar defect in the airfoil (option 2) led to the increase of total pressure losses by 0...7.3% in the range of angles of attack  $i > 29^\circ$  and its decrease by 0...14.6% at  $i < 29^\circ$ .

The airfoil thickness decrease (option 3) resulted in a reduction in the pressure loss value over the entire range of angles of attack. The maximum deviation between the initial and calculated values was 17.7% at the point  $i = 22^\circ$ . Along with the thickness decrease, the airfoil camber and the area of the friction surface have changed affecting the level of losses.

When the blade end sections were bended (options 4 and 5), both an increase and a decrease in the loss level were observed. At angles of attack  $i < 24^\circ$ , the losses were higher when the leading edge angle was reduced, and, on the contrary, the losses were lower compared to the initial airfoil when the trailing edge angle was increased. At the point  $i = 24^\circ$ , the level of loss was the same for all three airfoils, and at larger angles of attack the reduction of  $\beta_{1b}$  led to the decrease in level of losses by 3.9% at the point  $i = 33^\circ$ , while the increase of  $\beta_{2b}$  resulted in the increase of losses by 2.8% at the point  $i = 33^\circ$ .

A change in the angle of attack – flow turning angle relationship was observed for all the considered defects, which is mainly due to a change in the flow-delay angles. The pressure was also redistributed along the airfoil in its various regions. For example, with the leading edge thinning, the redistribution was observed in the initial region (up to  $0.1b$ ). When the thickness was changed, the redistribution took place on the suction side at  $(0.1...0.5)b$  and on the pressure side at  $(0.1...0.8)b$ .

It is worth noting that all the considered defects led to a shift in the optimal range of angles of attack, which corresponds to the minimum losses. This is often one of the reasons for incoherence of the blade vertical sections and stages in a multi-stage compressor, which negatively affects the GTU performance.

Having performed a series of numerical calculations with various axial compressor blade row defects and their combinations, a cluster analysis can be conducted in order to identify groups by the degree and nature of the defect influence on the characteristics of the axial compressor and GTU. Based on the correlation and regression analysis, it becomes possible to further identify relationships between the geometry of the same type of defects of different depths and the main performance parameters of the axial compressor and GTU.

## 5. Conclusion

Technical condition of the GTU axial compressor and other components is gradually decreasing while in service. The size of the blades, their surface condition, and the radial clearances are changing as a result of the operational processes, which results in axial compressor characteristics changes and reverses the GTU operating parameters as a whole. During inter-repair periods, manufacturers restore the blade row shape or replace it (partially or completely). At the same time, geometric deviations of certain axial compressor blades from the reference values occurring after the restoration and repair can also affect the level of output power, efficiency, and operational stability margin. In this regard, the task of predicting the GTU performance having certain information about deviations and defects of its certain components seems to be an important and promising one. A large number of different software systems available allows to find a solution not only to this, but also to some related problems.

The axial compressor blade algorithm presented in this paper, which allows to make local changes to blade geometry, is a basic component of a larger model under development that enables predicting the GTU performance with certain accuracy, taking into account various deviations. This model can be used for detecting blade defects and batching axial compressor at the stage of GTU repair, as well as for forecasting changes in GTU operating parameters when in service.



## 6. References

- [1] Gritsenko Y A and Idelson A M 1992 *New technological processes and reliability of GTE: Collection CIAM* (Moscow) 42-51
- [2] Komarov O V, Blinov V L, Sedunin V A and Skorochodov A V 2014 *Proceedings of ASME TurboExpo GT-2014-25392*
- [3] Rafikov L G and Ivanov, V A 1992 *Operation of the Gas-Compressor Equipment of Compressor Stations* (Moscow: Nedra Publishing House) P. 237
- [4] Revzin B S 2000 *Axial Compressors of Gas Turbine Gas Pumping Units: Study guide* (Ekaterinburg: USTU) P. 90
- [5] OST 1 02571-86 1987, *Compressor and Turbine Blades. Maximum Deviations of Sizes, Shapes, and Position of the Airfoil*
- [6] ISO 19859:2016, *Gas turbine applications – Requirements for power generation*
- [7] Marx J, Stading J, Reitz G and Friedrichs J 2014 *CEAS Aeronautical Journal* **5** 515-525
- [8] Ratkovska K, Hocko M 2017 *AIP Conference Proceedings* **1889:1** 20-31
- [9] Blinov V L 2015 *Development of the Principles of Parametric Profiling of blades flat cascade of GTU Axial Compressors Based on the Results of Multi-criteria Optimization* (Ekaterinburg: Yeltsin UrFU) P. 168
- [10] Nalimov Yu S 2014 *Ukraine Metal and Casting* **12(259)** 17-22
- [11] Tabakoff W, Hamed A and Shanov V 1998 *International journal of Rotating Machinery* **4:4** 233-241
- [12] Blinov V L, Brodov Yu M, Komarov O V and Sedunin A V 2015 *Energy Issues* **3-4** 86-95
- [13] Emery J C, Herrig L J, Erwin J R and Felix A R 1958 *Systematic two-dimensional cascade test of NACA 65-series compressor blades at low speeds: NACA Report 1368* (NACA)
- [14] Komarov O V, Blinov V L, Sedunin V A and Serkov S A 2016 *Vestnik BMSTU. Series "Engineering"* **1** pp 54-67
- [15] Blinov V L, Sedunin V A and Komarov O V 2019 *IOP Conf. Series: Materials Science and Engineering* **643**
- [16] Blinov V L, Sedunin V A, Serkov S A and Komarov O V 2016 *International Journal of Gas Turbine. Propulsion and Power Systems* **8:339-46**